Numerical evaluation of a second-order water transfer term for variably saturated dual-permeability models

J. Maximilian Köhne and Binayak P. Mohanty

Department of Biological and Agricultural Engineering, Texas A&M University, College Station, Texas, USA

Jirka Simunek

Department of Environmental Sciences, University of California, Riverside, California, USA

Horst H. Gerke

Center for Agricultural Landscape and Land Use Research, Institute of Soil Landscape Research, Müncheberg, Germany

Received 18 April 2004; accepted 26 May 2004; published 28 July 2004.

[1] Dual-permeability models contain a lumped mass transfer term that couples equations for water flow in the soil matrix and fracture systems. Linear first-order transfer terms cannot accurately calculate water transfer between the domains during early times of pressure head nonequilibrium. In this study, a second-order equation for water transfer into spherical rock matrix blocks [*Zimmerman et al.*, 1993, 1996] was adapted and evaluated comprehensively for water transfer into and out of variably saturated soil matrix blocks of different hydraulic properties, geometries, and sizes, for different initial and boundary conditions. Numerical solutions of the second-order term were compared with respective results obtained with a first-order term and a one-dimensional horizontal flow equation. Accurate results were obtained after implementing two modifications in the second-order term. First, the hydraulic conductivity was calculated as a weighted arithmetic average of conductivities that used pressure heads in matrix and fracture. For a time-variable pressure head boundary condition, a fixed weighting factor of 17 could be applied irrespective of texture, initial condition, and matrix block size up to 10 cm. Second, if direction of water transfer changed (to or from matrix), the initial pressure head was reset to the equilibrium pressure head at the time of transfer reversal. The modified second-order term was implemented into a dual-permeability model, which closely approximated reference results obtained with a two-dimensional flow model. For rectangular slab-type or comparable geometry of soil matrix, the modified second-order term considerably improves the accuracy of dual-permeability models to simulate variably saturated preferential flow in soil. *INDEX TERMS:* 1875 Hydrology: Unsaturated zone; 1866 Hydrology: Soil moisture; 1829 Hydrology: Groundwater hydrology; *KEYWORDS:* dual-permeability model, preferential flow, second-order transfer term

Citation: Köhne, J. M., B. P. Mohanty, J. Simunek, and H. H. Gerke (2004), Numerical evaluation of a second-order water transfer term for variably saturated dual-permeability models, *Water Resour. Res.*, *40*, W07409, doi:10.1029/2004WR003285.

1. Introduction

[2] For simulating water exchange between regions of contrasting hydraulic properties in a fractured porous medium, many dual-permeability models rely on a linear first-order, "Warren-Root"-type [*Warren and Root*, 1963] water mass transfer term that in its most general form can be written as

$$\Gamma_w = (1 - w_f) C_m \frac{d\bar{h}_m}{dt} = \alpha K_m (h_f - \bar{h}_m), \qquad (1)$$

where Γ_w [T^{-1}] is the horizontal water flux (volumetric flux per unit volume), w_f[ ] is the volume fraction of the fracture pore system, α [L^{-2}] is a first-order water transfer coefficient, K_m [$L\ T^{-1}$] is the hydraulic conductivity of the matrix pore region, h_f[L] is the pressure head of the fracture pore region, $\bar{h}_m$ [L] is the average pressure head of the matrix region, and C_m [L^{-1}] equal to $d\theta_m/d\bar{h}_m$ is the specific water capacity of the matrix, where θ_m is the water content in the matrix. A mathematical derivation of equation (1) was given, for instance, by *Zimmerman et al.* [1993, 1996].

[3] A first-order transfer term such as equation (1) suffers two drawbacks compared with the full description of flow using, e.g., Richards' equation. First, it is theoretically valid only for quasi-steady water transfer [*Zimmerman et al.*, 1993] and therefore underestimates highly transient transfer flux for early times [e.g., *Zimmerman et al.*, 1993; *Gerke and van Genuchten*, 1993a]. Second, in a lumped formulation such as equation (1), K_m needs to be evaluated as some block-averaged, effective hydraulic conductivity function of the pressure head in the matrix and fractures that best represents

0043-1397/04/2004WR003285$09.00

the conductivity of the actual pressure head profile at all times. *Gerke and van Genuchten* [1993a] evaluated the conductivity in equation (1) as an arithmetic average function of pressure heads in both matrix and fractures and scaled the first-order transfer term to match the exact solution at 50% of the cumulative horizontal infiltration. Moreover, they assumed an effective hydraulic conductivity at the fracture-matrix interface, K_a [L T^{-1}], affected by fracture coatings [*Gerke and van Genuchten*, 1993a], to obtain following modified first-order transfer term:

$$\Gamma_w = (1 - w_f) C_m \frac{d\overline{h}_m}{dt} = \alpha_{GvG} K_a (h_f - \overline{h}_m) \tag{2a}$$

$$\alpha_{GvG} = \gamma_w \frac{\beta}{a^2} \tag{2b}$$

$$K_a = 0.5 [K_a(h_f) + K_a(h_m)], \tag{2c}$$

where the transfer coefficient α_{GvG} includes the geometry-dependent coefficient β [ ], a dimensionless scaling factor γ_w, and the diffusion length a [L], representing the radius for spheres (or cylinders) or the half width for cubes (or rectangular plates). On average, a scaling factor γ_w of 0.4 was deemed to give best results. However, best fit scaling factors differed by up to 5 times for different initial pressure head values between -30 and -3000 cm and varied by 20% or less between medium and fine textured soils [*Gerke and van Genuchten*, 1993a, Tables 2 and 3]. Even for the best fit scaling factors, the relative cumulative horizontal infiltration was initially underestimated and later overestimated, revealing the inherent limitations of the first-order approach. A transfer term similar to equation (2) was subsequently used by *Gwo et al.* [1995] and *Ray et al.* [1997], among others.

[4] An accurate coupling term for a saturated dual-permeability system was suggested by *Dykhuizen* [1990]. The approach consisted of two different equations applicable to early- and late-time lateral imbibition. A nonlinear ordinary differential equation accurate for all times was presented by *Zimmerman et al.* [1993]. Their second-order water transfer term, derived by differentiating an analytical solution adapted from *Vermeulen* [1953], accurately approximates the exact solution for the pressure response of a spherical matrix block to a step function increase in the pressure head at its outer boundary [*Zimmerman et al.*, 1993]. The term was subsequently modified for variably saturated conditions [*Zimmerman et al.*, 1996] and in the notation of this paper is given by

$$\Gamma_w = (1 - w_f) C_m \frac{d\overline{h}_m}{dt} = \frac{\beta K_m}{2a^2} \frac{(\overline{h}_m - h_i)^2 - (h_f - h_i)^2}{(\overline{h}_m - h_i)}, \tag{3}$$

where t is time [T] and h_i [L] is the initial pressure head, i.e., a value that is assumed to be the same in the fractures and matrix being initially in equilibrium. The second-order term (3) closely approximated reference solutions of horizontal infiltration into saturated porous spheres and cubes [*Zimmerman et al.*, 1993]. For unsaturated horizontal infiltration into a 200-cm-thick rectangular rock slab, results obtained with the dual-permeability transport of unsaturated groundwater and heat (TOUGH) model with the second-order mass transfer term were also in excellent agreement with the numerical reference simulation. However, for structured soils, matrix aggregate sizes are much smaller than 200 cm while matrix hydraulic conductivities are generally much larger as compared with rock systems. It was also shown that diffusion for fundamentally different geometries like spheres and cylindrical macropores cannot be described with a single, geometry-based model [*van Genuchten and Dalton*, 1986; *Young and Ball*, 1997]. Hence it is not clear how the second-order term applies to an aggregated soil and to the geometry of a cylindrical macropore system.

[5] In this paper we will evaluate equation (3) with three modifications for flow in macroporous soil systems. The first modification is that for variably saturated water flow, K_m will be evaluated as a block-averaged, effective function henceforth denoted $\overline{K}_m$. No hydraulic resistance at the fracture-matrix interface will be assumed for $\overline{K}_m$ as opposed to K_a in equation (2). Second, to allow for variable directions of transfer between fracture and matrix with nonmonotonic variation of h_f, equation (3) is modified in a way that ensures that $d\overline{h}_m/dt$ always has the same sign as $(h_f - \overline{h}_m)$, as was shown and explained in detail by *Zimmerman et al.* [1993, Appendix B] for the saturated system. Third, the initial pressure head in equation (3) is considered to be a dynamic variable, h_i^d. Every time the transfer direction changes, h_i^d is reset to the pressure head value at the crossover point of matrix and fracture pressure heads, i.e., the equilibrium pressure head at the time of transfer reversal. With these modifications, equation (3) changes to

$$\Gamma_w = (1 - w_f) C_m \frac{d\overline{h}_m}{dt} = \frac{\beta \overline{K}_m}{2a^2} \frac{(h_f - \overline{h}_m)\left[\left|\overline{h}_m - h_i^d\right| + \left|h_f - h_i^d\right|\right]}{\left|\overline{h}_m - h_i^d\right|}. \tag{4}$$

[6] The primary objective of this study is to evaluate and enhance the accuracy of a second-order transfer term to improve predictions of dual-permeability models for variably saturated preferential flow in structured soils. The second-order mass transfer term (4) is evaluated in two steps. In the first step, water transfer predictions obtained with the first- and second-order transfer terms are compared with a reference numerical solution of a horizontal flow equation. Specific tasks with regard to the evaluation and improvement of the second-order term are (1) to analyze the effects of hydraulic properties, initial and boundary conditions, matrix size, and geometry, (2) to find the best single estimation scheme for $\overline{K}_m$, and (3) to improve predictions of the second-order term for variable transfer directions. In the second step, the performance of one-dimensional dual-permeability models with first- and second-order transfer terms is assessed by comparing their results with numerical reference solutions of the two-dimensional Richards' equation assuming different flow scenarios.

2. Comparison of the First- and Second-Order Mass Transfer Terms With Horizontal Flow Equation

2.1. Procedure

[7] In numerical dual-permeability models, water transfer between the matrix and fractures is assumed to be perpen-

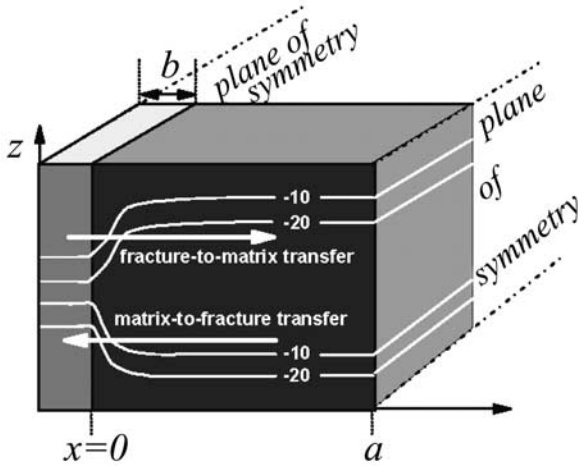

Figure 1. Schematic representation of an elementary unit of a dual-permeability system consisting of parallel rectangular matrix blocks of half-width a separated by fractures of half width b. White lines represent fictitious pressure heads.

dicular to the direction of flow and has to be calculated for each discretization element. Since preferential flow in soils typically tends to be vertical, water transfer is essentially horizontal. Therefore, as a starting point, water transfer calculated with the first- and second-order mass transfer terms will be compared with reference results obtained with the following equation describing the horizontal water flow in variably saturated rectangular matrix slabs:

$$\frac{\partial \theta_m(x,h_m)}{\partial t} = \frac{\partial}{\partial x}\left[K_m(x,h_m)\frac{\partial h_m(x,t)}{\partial x}\right] \quad 0 \le x \le a, \qquad (5)$$

where x [L] is the local horizontal coordinate between the fracture boundary at $x = 0$ and the center of a slab at $x = a$. Figure 1 shows a schematic representation of a corresponding dual-permeability medium. For the purpose of comparing transfer terms and the horizontal flow equation, the vertical flow direction indicated by the vertical axis in Figure 1 is neglected. A discretized form of equation (5) was numerically solved using HYDRUS-1D [*Simunek et al.*, 1998] with a very small element size of 0.05 cm. On the basis of results for θ_m in equation (5), effective values of the matrix pressure heads $\overline{h}$ were calculated from the average saturation of the matrix block $\overline{S_e}$, using the inverse of *van Genuchten*'s [1980] relation:

$$\overline{h} = \alpha^{-1}\left[\overline{S}_e^{\frac{n}{1-n}} - 1\right]^{\frac{1}{n}} \qquad (6a)$$

$$\overline{S}_e = \int_0^a \frac{\theta_m - \theta_{m,r}}{\theta_{m,s} - \theta_{m,r}} dx, \qquad (6b)$$

where $\theta_{m,r}$ and $\theta_{m,s}$ are the local residual and saturated water contents of the matrix, respectively, and α and n are empirical constants for the matrix (here without index m for better legibility of equation (6a)).

[8] For numerical solution, the first-order transfer term (2) and the second-order transfer term (4) are expressed in the following discretized forms (7) and (8) without the term $(1 - w_f)$ so that they can be directly compared with equation (5).

$$\frac{\Delta \overline{h}_m}{\Delta t} = \frac{0.4\beta \overline{K}_m}{a^2 \overline{C}_m}\left(h_f - \overline{h}_m\right) \qquad (7)$$

$$\frac{\Delta \overline{h}_m}{\Delta t} = \frac{\beta \overline{K}_m}{2a^2 \overline{C}_m}\frac{\left(h_f - \overline{h}_m\right)\left[\left|\overline{h}_m - h_i^d\right| + \left|h_f - h_i^d\right|\right]}{\left|\overline{h}_m - h_i^d\right|}. \qquad (8)$$

The nonlinear functions $\overline{C}_m$ and $\overline{K}_m$ were evaluated using the *van Genuchten* [1980] equations of the soil hydraulic properties. In equation (7), $\overline{K}_m$ is evaluated according to equation (2c) with K_a replaced by K_m. The first- and second-order mass transfer equations (7) and (8), respectively, were solved for $\overline{h}_m$ iteratively at each time step using Matlab (Mathworks, Inc.). Multiplying the solutions of equations (7) and (8) in terms of $\Delta \overline{h}_m/\Delta t$ with $\overline{C}_m$ provided the transfer flux Γ_w, which was compared to the solution of equation (5).

[9] To evaluate the second-order term, different textures, initial conditions, matrix sizes, and boundary conditions were assumed, initially limiting the analysis to rectangular slab-type geometry of matrix blocks. Geometry was represented by a factor β in equations (7) and (8). Values for β in equation (7) could be derived, for example, by comparing the solution of the first-order transfer term, assuming a certain geometry and a step-function boundary condition, with a Laplace transform of the linearized horizontal water flow equation (e.g., β equals 3 for slab-type matrix blocks) [*Gerke and van Genuchten*, 1993a]. By analogy, the same β values were used in equation (8).

[10] For the standard scenario, rectangular slab-type ($\beta = 3$) matrix blocks with a half width a of 5 cm were considered. Two values of h_i, equal to -100 and -1000 cm, were selected for initial conditions. To represent the matrix soil hydraulic properties, *van Genuchten* [1980] parameters representing textures "silty clay," "silt," and "loamy sand" were chosen from a database of *Carsel and Parrish* [1988] (Table 1). The following expressions for calculating the effective hydraulic conductivity, $\overline{K}_m$, in equation (8) were used:

Matrix $$\overline{K}_m = K_m(h_m) \qquad (9a)$$

Fracture $$\overline{K}_m = K_m\left(h_f\right) \qquad (9b)$$

Arithmetic $$\overline{K}_m = \left(K_m(h_m) + K_m\left(h_f\right)\right)/2 \qquad (9c)$$

Geometric $$\overline{K}_m = \left(K_m(h_m)K_m\left(h_f\right)\right)^{0.5} \qquad (9d)$$

Integral $$\overline{K}_m = \frac{1}{h_f - h_m}\int_{h_m}^{h_f} K_m(h)dh \qquad (9e)$$

Table 1. *Van Genuchten* [1980] Parameters Used for Horizontal, Two-Dimensional, and Vertical Dual-Permeability Flow Simulations[a]

	θ_r	θ_s	α, 1/cm	n	K_s, cm/d
Silty clay	0.070	0.36	0.005	1.09	0.48
Silt	0.340	0.46	0.016	1.37	6.0
Sandy loam	0.065	0.41	0.075	1.89	106.1
Sand	0.045	0.36	0.145	2.68	712.8

[a]Parameters from *Carsel and Parrish* [1988].

When the *van Genuchten* [1980] model is used to calculate K_m, the integral approach (9e) requires numerical integration. Hence, for each time step within the numerical solution of equation (8), equation (9e) was itself numerically solved utilizing an integral, adaptive Simpson quadrature as implemented in the Quad routine of Matlab (Mathworks, Inc.). Note that for consistency, $\overline{C}_m$ was always evaluated with the same respective scheme as $\overline{K}_m$. Evaluation of $\overline{C}_m$ affects the prediction of $\overline{h}_m$ but not of transfer flux, Γ_w.

[11] Statistical analysis was performed for results of different approaches subject to the step-increase boundary condition in order to select the most appropriate approach for further analyses using transient boundary condition. The root-mean-square error (RMSE), quantifying deviations between observations O_i (horizontal flow equation solution) and estimates E_i (mass transfer term solution), was calculated and normalized with the arithmetic mean of observations, $\overline{O}$, to yield a normalized RMSE or coefficient of variation (CV) [*Green and Stephenson*, 1986]:

$$CV[\%] = \frac{100}{\overline{O}} \left(\frac{\sum_{i=1}^{n} (O_i - E_i)^2}{n} \right)^{1/2} = \frac{100}{\overline{O}} RMSE \qquad (10)$$

2.2. Results for the Fracture-to-Matrix Transfer Using a Step-Increase Boundary Condition

[12] The following initial condition and step-increase boundary conditions were assumed for the horizontal flow equation (5):

$$h_m(x, t = 0) = h_i \qquad (11a)$$

$$h_m(x = 0, t > 0) = h_0 \qquad (11b)$$

$$q(x = a, t \geq 0) = 0, \qquad (11c)$$

where equation (11c) implies zero flow across the midplane of rectangular slabs. For water transfer terms (7) and (8), the corresponding initial and boundary conditions were

$$\overline{h}_m(t = 0) = h_f(t = 0) = h_i \qquad (12a)$$

$$h_f(t > 0) = h_0. \qquad (12b)$$

Since the water transfer terms are spatially nondimensional, ordinary differential equations, equation (12b) is only a conceptual boundary condition. Practically, equation (12b) means that h_f in equations (7) and (8) was kept constant when solving the initial value problem.

[13] Simulated water transfer at the initial pressure head of -1000 cm is shown in Figure 2. Note the decrease in timescale and increase in total water transfer from silty clay, silt, to sandy loam. Using the matrix approach (8a), the second-order model significantly underestimated cumulative transfer for all textures (Figure 2). The estimation somewhat improved with finer texture, characterized by smaller hydraulic conductivity. This may explain why *Zimmerman et al.* [1996] found an excellent agreement between the second-order model and the numerical reference simulation of unsaturated horizontal imbibition into a rock slab. *Zimmerman et al.* [1996] considered the saturated hydraulic conductivity of rock matrix 4 orders of magnitude smaller than K_m of our silty clay.

[14] The second-order term with the fracture approach (9b) overestimated the water transfer (Figure 2) with CV values smaller than those for the matrix approach (Table 2). Only minor improvements were gained with the arithmetic approach (9c) that provided predictions relatively close to the fracture approach (Figure 2). The geometric approach (9d) revealed the strongest sensitivity to a change in texture (Figure 2). The best overall approximation, relatively independent of texture, was achieved with the integral approach (9e) (Figure 2, Table 2). The scaled first-order transfer model (2) always overestimated water transfer (Figure 2). Only for sandy loam (Figure 2c) was the agreement relatively good with a comparably low CV value (Table 2). No approach satisfactorily described the reference solution for all three textures.

[15] Figure 3 shows results for the initial pressure head of -100 cm. The reference curve was somewhat better matched by all approaches and particularly by the first-order term (2). The CV values of most approaches were smaller for the initial pressure head of -100 cm than for -1000 cm, which shows that the variably saturated transfer term predictions improve for smaller pressure head gradients between the domains. Still better results were found for the initial pressure head of -10 cm (not shown).

[16] Using scaling factors as described by *Gerke and van Genuchten* [1993a] to match the dimensionless cumulative transfer at 0.5 with the second-order term yielded results only slightly better than the first-order term (2) for all three soils and both initial conditions of -100 and -1000 cm (not shown). Therefore the scaling approach was not considered further. Instead, in order to better match both early- and late-time water transfers, we tested the following weighted arithmetic averaging scheme for evaluating $\overline{K}_m$:

$$\text{Weighted arithmetic} \quad \overline{K}_m = \left(pK_m(h_m) + K_m\left(h_f\right)\right)/(p + 1), \qquad (13)$$

where p is a weighting factor calibrated to achieve the best fit to the reference model (5). Excellent agreement between the results obtained with the second-order term using the weighted arithmetic scheme (13) and the cumulative reference water transfer (Table 2) could be achieved during the entire time range for both initial conditions of -1000 and -100 cm and all textures (Figures 4 and 5). Note that no considerable improvement over the scaling approach of *Gerke and van Genuchten* [1993a] could be obtained by

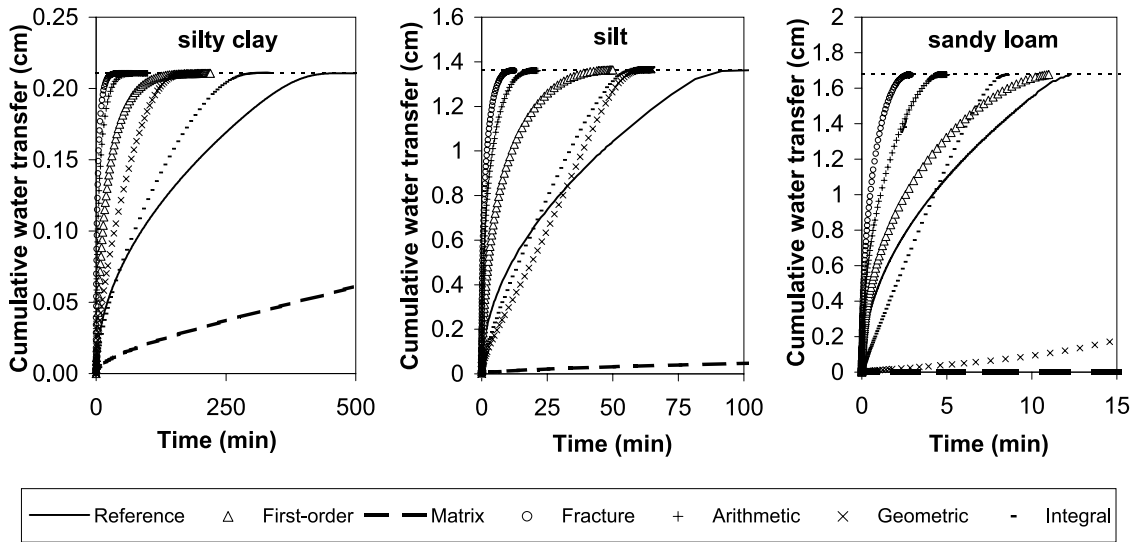

Figure 2. Cumulative water transfer into silty clay, silt, and sandy loam matrix slabs of 5-cm half width at the initial pressure head of −1000 cm for a step increase of the boundary pressure head to 0 cm. Simulation results are for the horizontal flow equation (5) (denoted "reference" in the legend), the first order-term (7) (denoted "first-order"), and the second-order term (8) with different evaluation schemes for $\overline{K}_m$ (matrix, fracture, arithmetic, geometric, and integral, corresponding to equations (9a), (9b), (9c), (9d), and (9e), respectively).

implementing the weighted arithmetic scheme (13) into the first-order transfer term (7) (results not shown).

[17] For the second-order term, the weighting factor p varied between 8 (sandy loam) and 59 (silty clay) (Table 2). This variation of p with texture can be explained to some degree by comparing the progression of the horizontal distributions of pressure heads and hydraulic conductivities with time. For the initial pressure head of −1000 cm, Figure 6 shows horizontal profiles of pressure heads and relative hydraulic conductivity calculated with the reference approach (5) for different fractions of the maximum time t_{max}, defined as the time when simulated pressure heads exceeded −0.005 cm in the entire profile. Pressure head increase became more abrupt in the textural order of silty clay, silt, and sandy loam, leading to sharp hydraulic gradients in the sandy loam. For similar positions of the pressure front, the hydraulic conductivity dropped faster from its maximum value at the (fracture) boundary for silty clay than for silt and sandy loam. Hence, for horizontal infiltration into a fine-textured porous medium assuming a step-increase boundary condition, "effective" hydraulic conductivity can be expected to depend more on pressure heads inside the domain than at the (constant head) fracture boundary. This phenomenon is particularly significant for fine textured soils and less so for coarse textured soils, which is reflected by decreasing p values in the order silty clay, silt, and sandy loam (Table 2).

2.3. Results for the Fracture-to-Matrix Transfer Using a Variable-Head Boundary Condition

[18] The step-type boundary conditions (11b) and (12b) represented only an approximation of the real process, since pressure heads in capillary fractures do not change in steps. In our subsequent simulations, the imposed pressure head at the boundary, h_0, in the boundary conditions (11b) and (12b) was assumed to be a time-dependent function, $h_0(t)$. The values for $h_0(t)$ were generated using the HYDRUS-1D simulations of infiltration at the zero pressure head upper boundary condition into a vertical, 80-cm-deep highly permeable porous medium, conceptually representing a "fracture system," being initially at either −1000 or −100 cm pressure head. A 30-min time series of the simulated pressure heads at 40-cm depth was taken as

Table 2. Coefficients of Variation Between Numerical Solutions of Horizontal Flow Equation (5) and the Second-Order Term (7) With Different Estimation Methods for $\overline{K}_m$ as Given by Equations (9a)–(9e) and (12), and Between Equation (5) and the First-Order Term (6)

	Coefficient of Variation, %							
	Matrix	Fracture	Arithmetic	Geometric	Integral	Weighted Arithmetic	p [ ]	First-Order
				h_i = −1000 cm				
Silty clay	1899	84.4	73.4	42.3	16.9	3.1	59	45.5
Silt	5238	77.0	71.2	19.3	22.0	4.1	29	44.4
Sandy loam	533300	71.5	57.8	2948.0	24.9	3.7	8	19.8
				h_i = −100 cm				
Silty clay	20	46.9	44.5	30.5	15.9	1.0	45	11.5
Silt	85	63.0	49.5	35.1	27.0	2.4	19	6.5
Sandy loam	8460	64.7	81.7	58.5	26.5	3.6	8	6.4

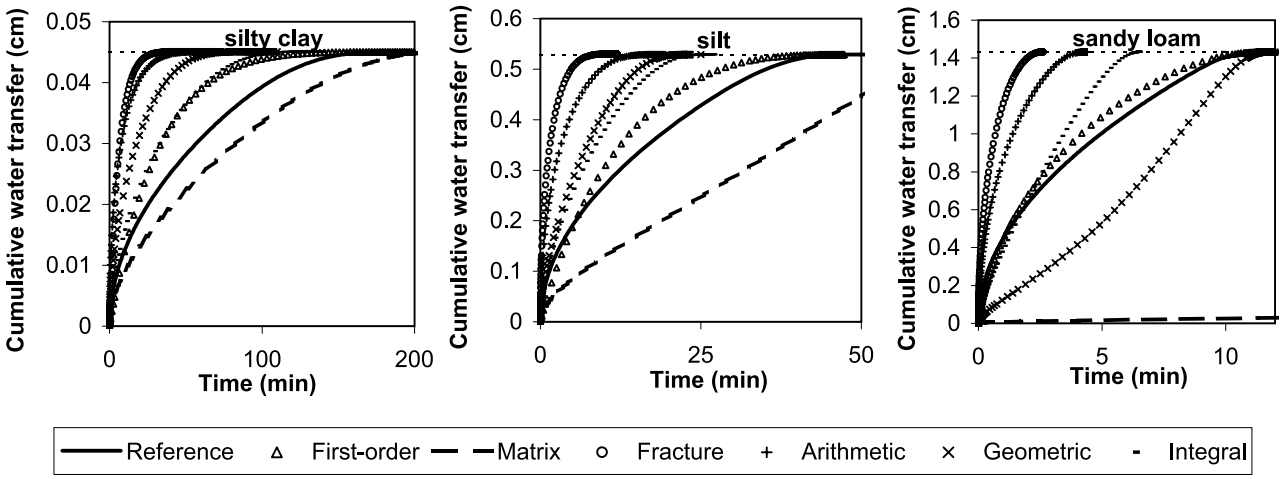

Figure 3. Same as Figure 2, but for the initial pressure head of −100 cm.

$h_0(t)$ in equations (11b) and (12b) for water transfer into the matrix blocks. This procedure gives values for $h_0(t)$ similar to those that would be obtained for the fracture region of a dual-permeability model with zero or negligible transfer into the matrix. In this way, the $h_0(t)$ values represent the most abrupt, "worst-case" increase of fracture pressure heads to be expected under natural conditions. Figure 7 shows the $h_0(t)$ boundary condition values rising from −1000 to 0 cm in less than 10 min and the matrix pressure head response calculated with the reference model (5) (reference-h). The figure also shows the relative water transfer estimated with equations (5) (reference-q), (7), and (8) in terms of the cumulative transfer normalized with the total transfer necessary to obtain full saturation.

[19] The reference matrix pressure heads rose faster in silt than in silty clay (Figure 7) due to faster water transfer into the more conductive silt. The first-order approach (7) did not match well with the relative water transfer for either texture (Figure 7). Similarly, the second-order term with the matrix, fracture, geometric, and arithmetic approaches failed to describe the reference curves, while the integral approach gave a good approximation for silty clay but not for silt (not shown). On the average, the second-order term with the weighted arithmetic scheme and p = 17 most accurately described water transfer into silty clay and silt (Figure 7). For the initial pressure head of −100 cm, best agreement was also found for p = 17 (Figure 8). Note that the $h_0(t)$ values increase rather suddenly close to saturation between −3 and 0 cm, since no matrix transfer was considered in the derivation of $h_0(t)$. This sudden increase causes deviations of the first-order term results from the reference curve for silty clay but not so much for silt (Figure 8) since between −3 and 0 cm, hydraulic conductivity increases tenfold for silty clay but only twofold for silt. Only minor deviations of the second-order term results were observed (Figure 8).

[20] The value of the empirical weighting factor p most likely cannot be derived theoretically. However, for different textures and initial conditions, values of p around 17 were obtained for step-increase boundary condition in the reference model, provided that the second-order term was solved with a variable-head boundary condition employing the simulated pressure head values in the reference model

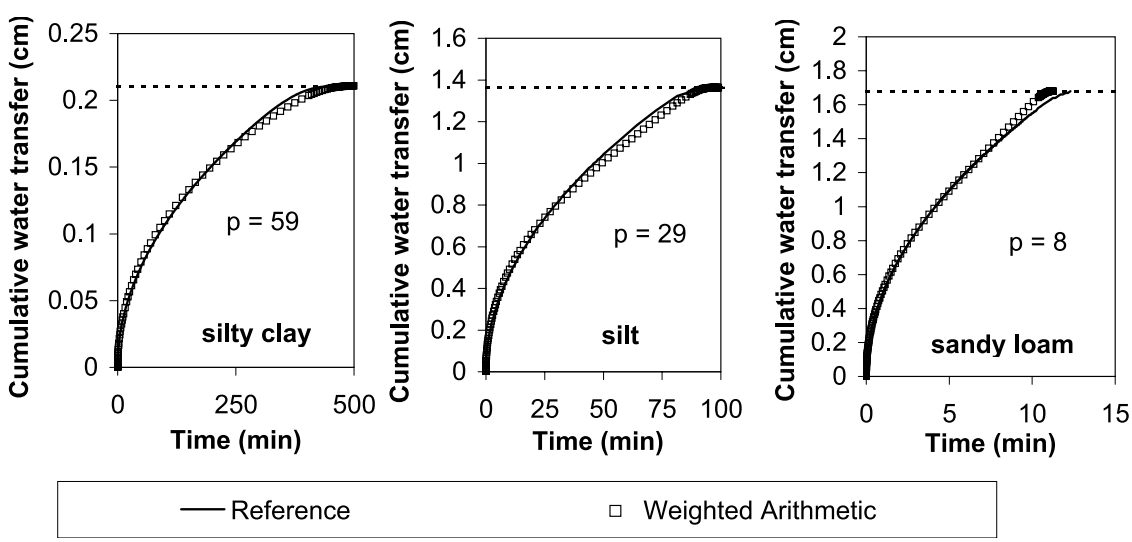

Figure 4. Same as Figure 2, but only simulation results for the horizontal flow equation (5) ("reference"), and the second-order term using $\overline{K}_m$-evaluation scheme (13) ("weighted arithmetic").

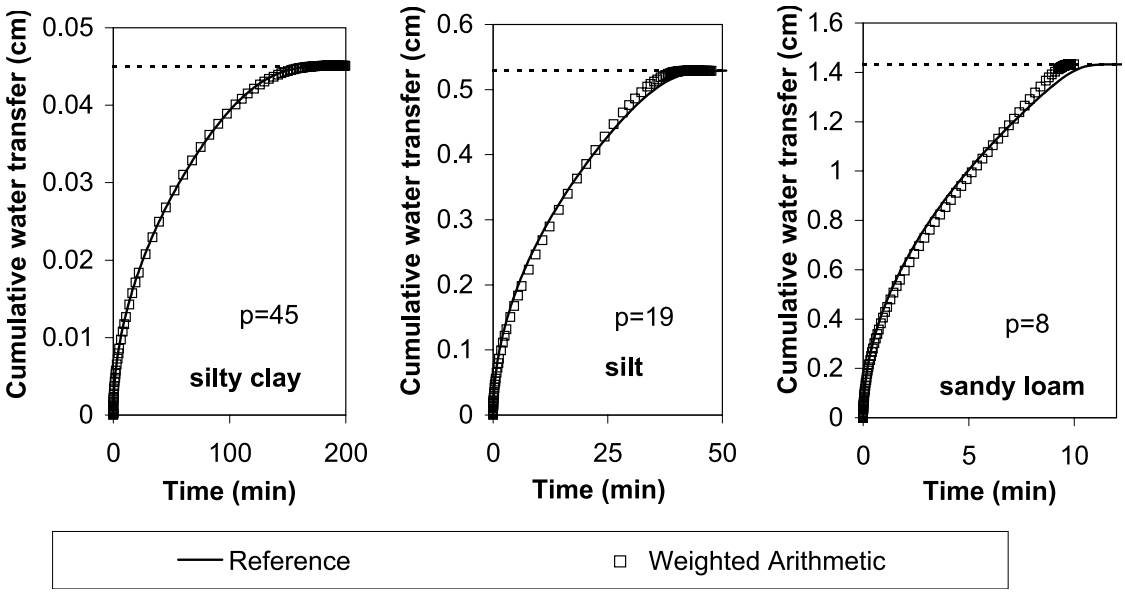

Figure 5. Same as Figure 4, but for the initial pressure head of −100 cm.

domain at the first numerical node just inside of the (fracture) boundary (results not shown). Hence a continuous instead of sudden pressure head increase at the boundary strongly reduces the dependence of p on texture and initial condition.

2.4. Results for Matrix-to-Fracture Transfer

[21] To date, studies on soil water transfer have focused only on fracture-to-matrix transfer. However, during drainage and evaporation periods, matrix-to-fracture transfer may be more important. We analyzed water transfer, or horizontal drainage, from an initially saturated matrix block subject to a variable-head boundary condition at the fracture face. On the basis of the fracture continuum concept [e.g., *Dykhuizen*, 1990; *Zimmerman et al.*, 1993], our approach assumes continuous water retention and hydraulic conductivity functions in a fracture continuum sustaining negative pressures during matrix-to-fracture transfer. Such a fracture

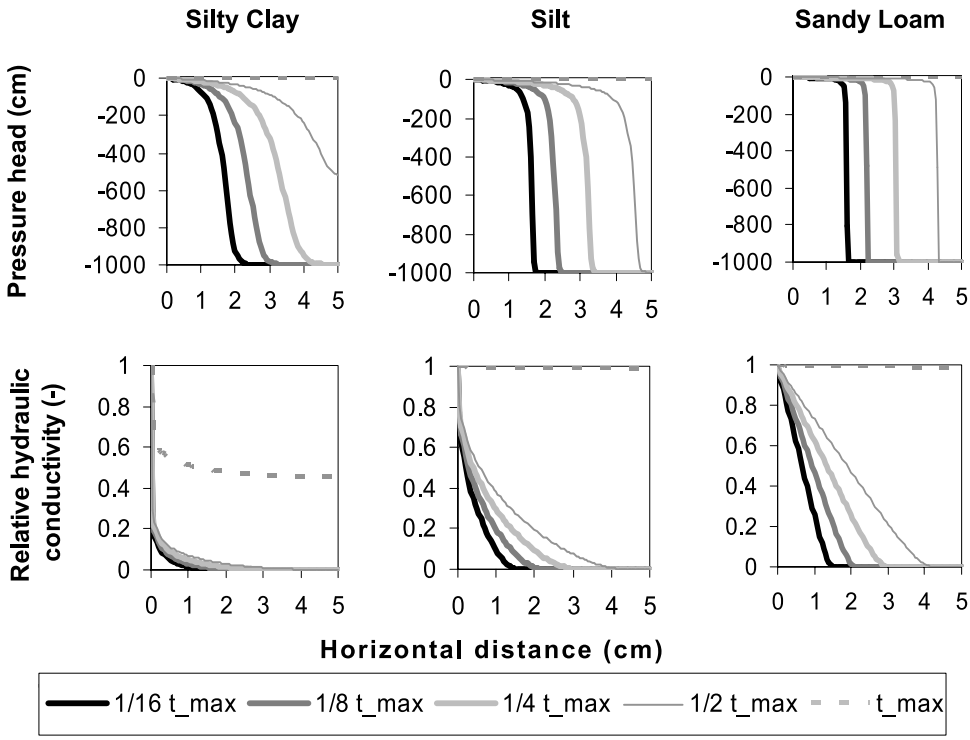

Figure 6. Simulation results for the horizontal flow equation (5) of pressure heads and relative hydraulic conductivities for cumulative water transfer into silty clay, silt, and sandy loam matrix slabs of 5-cm half width at the initial pressure head of −1000 cm for a step increase of the boundary pressure head to 0 cm. Graphs represent results at 1/16, 1/8, 1/4, 1/2, and 1 of the respective simulation time t_{max}.

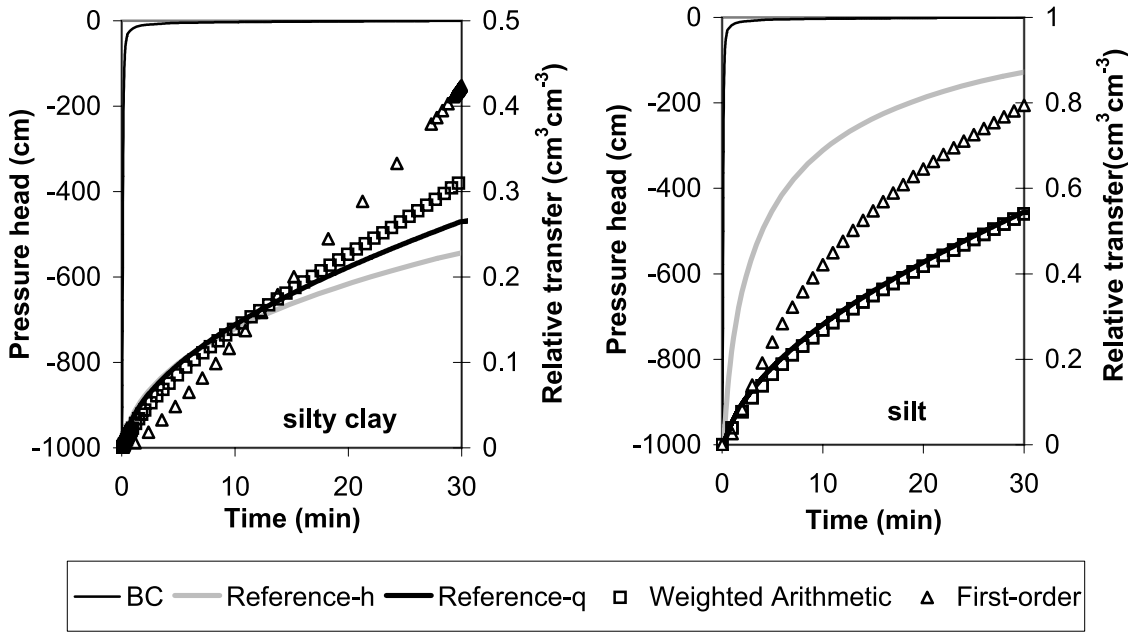

Figure 7. Cumulative water transfer into silty clay and silt matrix slabs of 5-cm half width with the initial pressure head of −1000 cm and increasing boundary pressure heads: the boundary pressure head (BC) and the average matrix pressure head calculated using the horizontal flow equation (5) (“reference-h”); and water transfer calculated using the horizontal flow equation (5) (“reference-q”), the first order-term (7) (“first-order”), and the second-order term (8) using the weighted arithmetic scheme (13).

continuum may physically represent a fracture network or a soil fracture pore system (or macropore) partially refilled with loose soil materials. We once again assumed rectangular slab geometry and 5-cm half width. The $h_0(t)$ values for boundary conditions (11b) and (12b) were generated by simulating 10 days of drainage at a constant evaporation rate of 0.3 cm/d from a vertical, 80-cm-deep, initially saturated fracture system using HYDRUS-1D. Simulated pressure heads at 2-cm depth below the evaporation boundary were taken as $h_0(t)$ in equations (11b) and (12b). Again, $h_0(t)$ values represent the fastest likely reaction of fracture pressure heads under conditions of drainage and evaporation. Figure 9 shows $h_0(t)$ values applied as a boundary condition for water transfer out of initially saturated matrix slabs, the average matrix pressure head response calculated with the reference model (5) using equation (6), and the cumulative matrix-to-fracture transfer as calculated with equations (5), (7), and (8) and normalized with the reference solution at 10 days. Average matrix pressure heads were relatively close to the fracture pressure heads, especially for

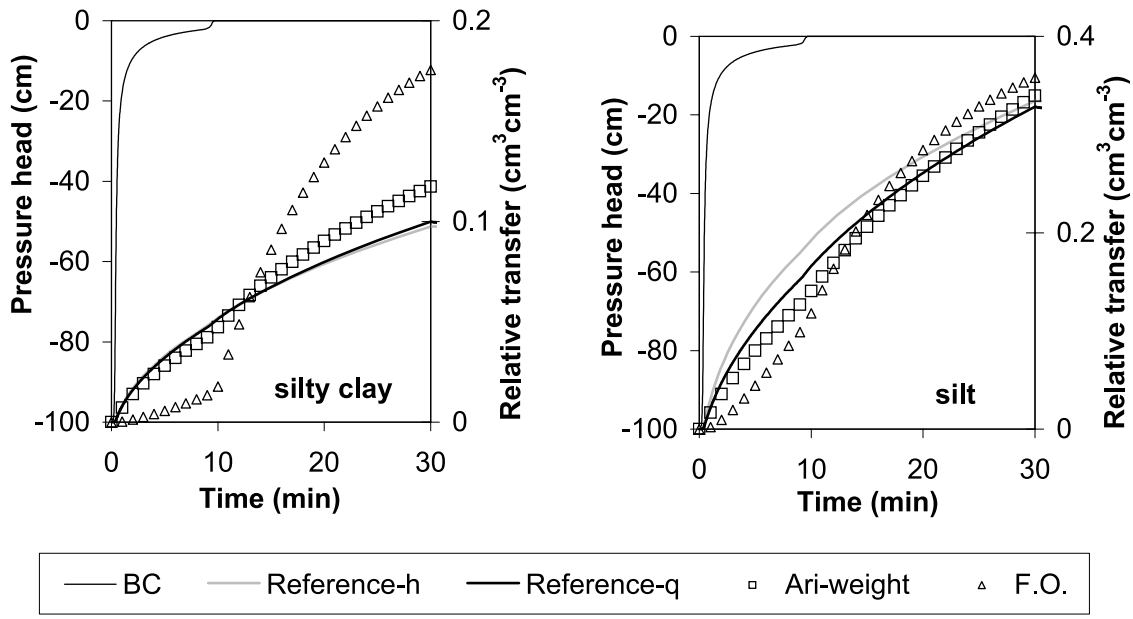

Figure 8. Same as Figure 7, but with the initial pressure head of −100 cm.

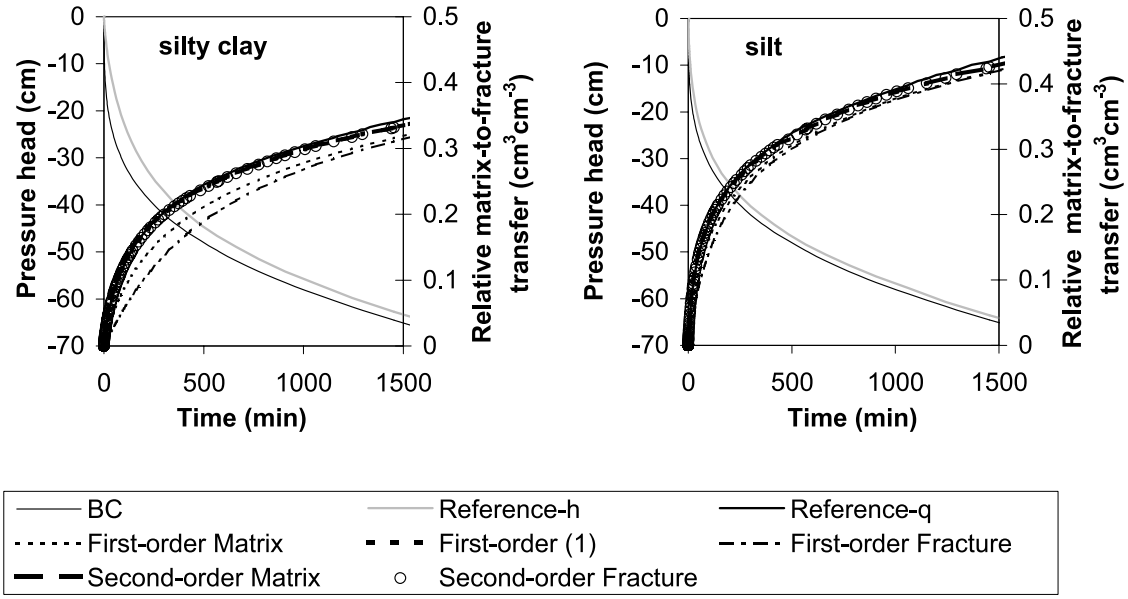

Figure 9. Matrix-to-fracture water transfer for initially saturated silty clay and silt matrix slabs of 5-cm half width: the boundary pressure head (BC) and the average matrix pressure heads calculated using the horizontal flow equation (5) (''reference-h''); and matrix-to-fracture water transfer calculated using the horizontal flow equation (5) (''reference-q''), the second-order term (8) using $\overline{K}_m$-evaluation schemes (9a) (''second-order matrix'') and (9b) (''second-order fracture''), and the first-order term (1) (''first-order (1)'') and (7) using $\overline{K}_m$-evaluation schemes (9a) (''first-order matrix'') and (9b) (''first-order fracture'').

silt (Figure 9). During matrix-to-fracture transfer, there was only mild hydraulic nonequilibrium as compared with fracture-to-matrix transfer, where differences between matrix and fracture pressure heads were much larger (see Figure 8). For both first- and second-order terms, only results for matrix (9a) and fracture (9b) based K_m evaluation schemes are shown, as all other approaches yielded results in between these two. The second-order term with the matrix and fracture schemes, as well as the original first-order term (1) without scaling coefficient, gave excellent approximations of the reference solution of equation (5) for both silty clay and silt (Figure 9). The first-order term (7) with γ_w equal to 0.4 [*Gerke and van Genuchten*, 1993a] underestimated matrix-to-fracture transfer (Figure 9). This means that the scaling factor γ_w only improves the first-order term description of fracture-to-matrix transfer, while it is not applicable to matrix-to-fracture transfer. The direction-dependent use of γ_w is similar to a pseudohysteresis in the first-order model.

2.5. Results for Reversible Water Transfer Between the Fracture and the Matrix Domain

[22] First- and second-order transfer terms were evaluated for ''field-like'' conditions with changing water transfer (matrix-to-fracture or fracture-to-matrix) directions. The boundary pressure heads were again calculated using HYDRUS-1D. The scenario (Figure 10) included 30-min water transfer into the silty clay matrix slab initially at −100 cm, followed by matrix-to-fracture transfer for 14400 min (10 days), and later water transfer back into the matrix for the last 60 min. The prediction using the first-order term underestimated, while the second-order term with the weighted arithmetic scheme (p = 17) matched the first fracture-to-matrix transfer (Figure 10a). Although boundary condition or fracture pressure heads decreased after 30 min, they remained larger than the average matrix heads for some time, and water transfer back into the fracture was delayed (Figure 10a). For the second fracture-to-matrix water transfer event that started after 10 days at the pressure head of −230 cm (Figure 10b), the second-order term (8) with the weighted arithmetic scheme (13) matched the reference solution poorly because the initial pressure head h_i was fixed at the original value of −100 cm. When h_i was adjusted to the new initial value (−230 cm), the result was in excellent agreement with the reference solution (Figure 10b). Hence the assumption underlying the second-order term of pressure head equilibrium between matrix and fracture continuum at the time of transfer reversal, while simplified with respect to the actual matrix pressure head profile (not shown), evidently allows a close approximation of the real process.

2.6. Effect of Matrix Block Size on Water Transfer Results

[23] We analyzed the sensitivity of the second-order transfer term with the weighted arithmetic scheme to the size of rectangular slabs. Figure 11 shows results for water transfer into silty clay matrix blocks with half widths of 1, 5, and 10 cm. In general, the second-order transfer term approach was more accurate than the first-order transfer term approach. Results for the second-order term with the weighted arithmetic scheme (13) came close to the reference solution for the smaller half widths, whereas agreement deteriorated for large matrix blocks of 20-cm diameter (Figure 11). The poor agreement was caused mainly by the boundary pressure heads increasing steeply from −3 cm to zero. Changing the weighting factor p from 17 to 59 at this intermediate step of pressure increase as discussed in the previous section (the value of 59 being calibrated for water transfer subject to a step-increase boundary condition)

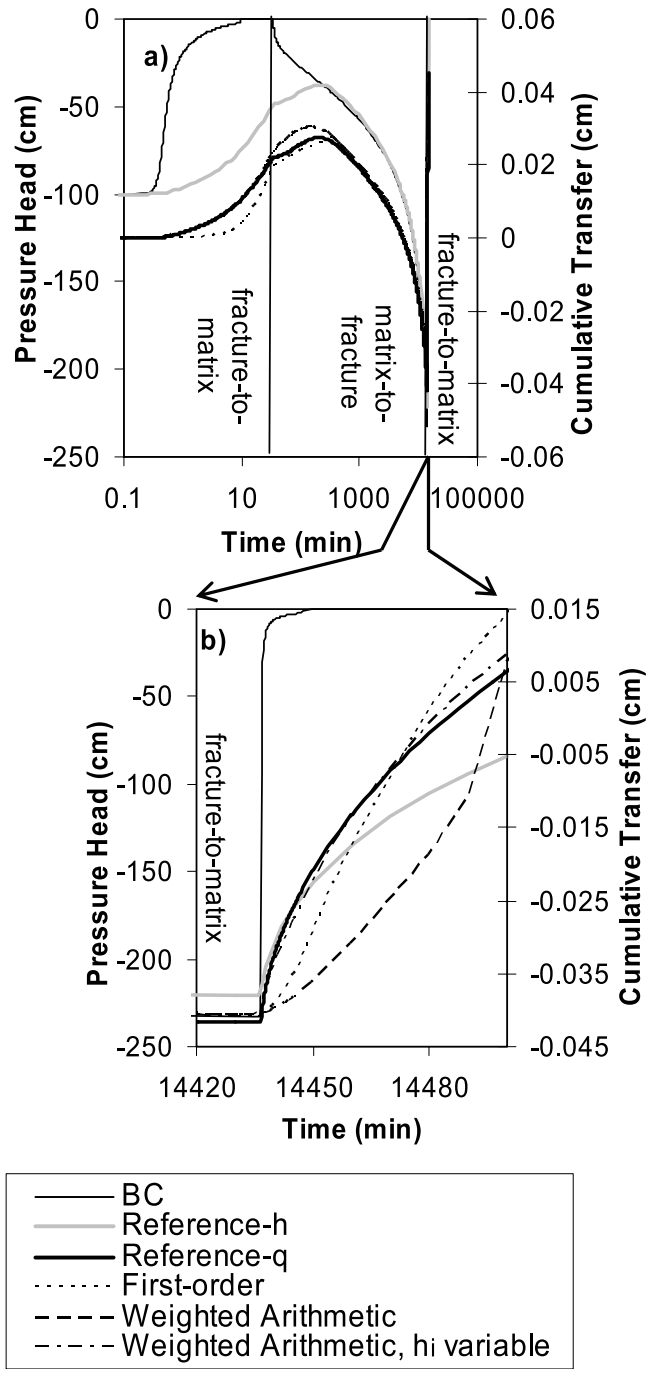

Figure 10. Cumulative water transfer for silty clay matrix slabs of 5-cm half width for a scenario with variable boundary pressure heads: the boundary pressure head (BC) and the average matrix pressure head calculated using the horizontal flow equation (5) (“reference-h”); and water transfer calculated using the horizontal flow equation (5) (“reference-q”), the first-order term (7) (“first-order”), and the second-order term (8) using evaluation scheme (13) with $p = 17$ (“weighted arithmetic” and “weighted arithmetic, h_i variable”). In the h_i variable scheme, the initial head in equation (8) was reset at 14,436 min to the simulated pressure head at that time. (a) Entire experiment duration. (b) Results for time interval from 14,420 to 14,500 min.

improved weighted arithmetic simulation (Figure 11) but is not a feasible modeling scheme. However, for most field soils, the half width of aggregates will be smaller than 10 cm, justifying the use of a constant weighting factor in the weighted arithmetic scheme.

3. Evaluation of the Second-Order Transfer Term in a Dual-Permeability Model

3.1. Procedure

[24] The second-order transfer term with the weighted arithmetic approach (13) with $p = 17$ was evaluated with regard to its effect on dual-permeability model simulations of preferential flow. The dual-permeability model of *Gerke and van Genuchten* [1993b] as implemented into HYDRUS-1D [*Simunek et al.*, 2003] uses two mixed-type Richards' equations to describe water flow in the fractures (14a) and the matrix (14b):

$$\frac{\partial \theta_f}{\partial t} = \frac{\partial}{\partial z}\left(K_f \frac{\partial h_f}{\partial z} + K_f\right) - \frac{\Gamma_w}{w_f} \tag{14a}$$

$$\frac{\partial \theta_m}{\partial t} = \frac{\partial}{\partial z}\left(K_m \frac{\partial h_m}{\partial z} + K_m\right) + \frac{\Gamma_w}{1 - w_f}. \tag{14b}$$

A positive mass transfer term Γ_w denotes the fracture-to-matrix transfer, while a negative Γ_w signifies the matrix-to-fracture transfer. The system of two dual-permeability flow equations for matrix and fracture was solved sequentially, first for the matrix and then for the fracture pore system, using the method of finite differences. The volume fraction of the fracture pore system, w_f, was calculated depending on geometry as follows:

$$w_f = \frac{b}{a+b} \qquad \text{parallel plates,} \tag{15a}$$

$$w_f = \frac{b^2}{(a+b)^2} \qquad \text{hollow cylindrical macropore,} \tag{15b}$$

where a [L] is the half width of the matrix and b [L] is the half width of the fracture or the radius of a cylindrical macropore. For a dual-permeability medium consisting of cylindrical macropores surrounded by soil matrix, the following expression was adopted to calculate β [*Gerke and van Genuchten*, 1996] in transfer terms (2) and (4):

$$\beta = \frac{1}{[0.19 \ln(16\varsigma_0)]^2}; \quad 1 < \varsigma_0 < 100 \tag{16a}$$

$$\varsigma_0 = (a+b)/b, \tag{16b}$$

where ζ_0 [ ] is the outer-to-inner-radius ratio of the hollow cylinder. The transfer terms (2) and (4) were implemented into the dual-permeability model. As a reference model, we applied the two-dimensional numerical model HYDRUS-2D [*Simunek et al.*, 1999] to a transport domain with two vertical layers representing the matrix and fracture regions

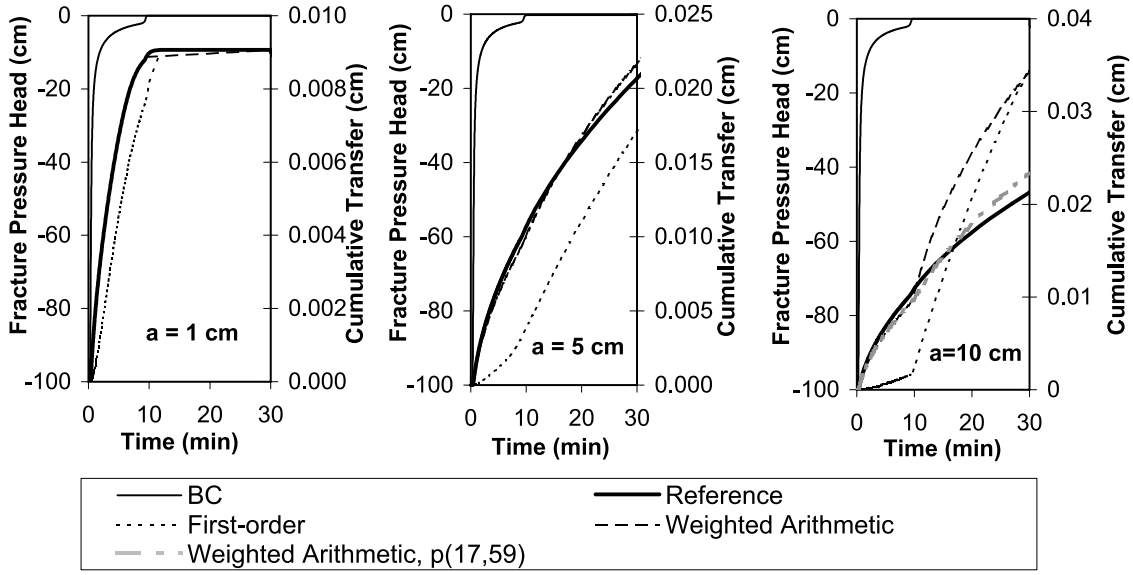

Figure 11. Cumulative water transfer into silty clay matrix slabs with half width a = 1 cm, a = 5 cm, and a = 10 cm for a scenario of variable fracture pressure heads (BC) calculated using the horizontal flow equation (5) (“reference”), the first-order term (7) (“first-order”), and the second-order term (8) using evaluation scheme (13) with p = 17 (“weighted arithmetic”) and with p changing from 17 to 59 at 10 min (“weighted arithmetic, p(17, 59)”).

(Figure 12). HYDRUS-2D solves the mixed-type Richards equation in two dimensions using the Galerkin finite element method. We modified HYDRUS-2D to calculate water transfer across the interfaces between two vertical layers using a procedure similar to that for fluxes through the boundary nodes with prescribed Dirichlet boundary conditions [*Simunek et al.*, 1999]. Nodal fluxes are calculated from a finite element matrix equation that is obtained by discretization of the Richards equation and assembled for all elements on one side of the interface. The finite element matrix equation for internal fluxes is calculated at the last iteration after convergence for given time level had been achieved. Fluxes calculated directly from the Richards equation are much more accurate than fluxes calculated using Darcy’s law and have the same accuracy as the overall solution.

[25] Five scenarios as defined in Table 3 were selected assuming an 80-cm-deep vertically structured soil profile. The fracture system was represented by “sand” with van Genuchten parameters given in Table 1 and was assigned a half width b of 0.25 cm. A seepage face lower boundary condition was assumed.

3.2. Results

3.2.1. Infiltration Into a Parallel-Slab-Type Dual-Permeability Medium With the Silty Clay Matrix (Scenario 1)

[26] Figure 13a shows the depth profiles of water transfer Γ_w at 15 and 60 min during infiltration as simulated using the dual-permeability model (DPM) with first- and second-order mass transfer term and HYDRUS-2D assuming a dual-permeability medium consisting of a silty clay matrix with slab geometry adjacent to a fracture (see Figures 1 and 12). The Γ_w profiles at both 15 and 60 min were similar for HYDRUS-2D and the second-order DPM, whereas the first-order DPM failed to describe high peak values of Γ_w near the infiltration front (Figure 13a).

3.2.2. Effect of the Silt Matrix (Scenario 2)

[27] The assumption that the matrix consisted of silt instead of silty clay (in scenario 1) resulted into a significantly slower vertical movement of the moisture front, since the larger hydraulic conductivity of silt caused larger water transfer rates into the matrix (Figure 13b). However, water transfer in both two-dimensional and dual-permeability model simulations was reduced to zero about 20 cm above the infiltration front (Figure 13b). In this region, complete equilibration between pressure heads in fracture and matrix was obtained due to large transfer rates. Both first- and second-order DPMs gave satisfactory approximations of the

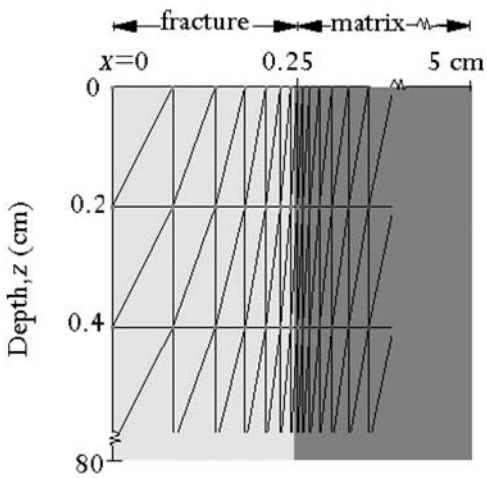

Figure 12. Finite element grid used in the two-dimensional reference simulations.

Table 3. Scenarios Used in HYDRUS-2D and the Dual-Permeability Model for Evaluating First- and Second-Order Water Transfer Terms[a]

Scenario	Flow Process	Geometry	Matrix Texture[b]	h_i,[c] cm	a, cm	β	w_f	Upper Boundary Condition
1	infiltration	rectangular	silty clay	−100	5	3	0.0476	$h = 0$
2	infiltration	rectangular	silt	−100	5	3	0.0476	$h = 0$
3	infiltration	hollow cylindrical	silty clay	−100	5	0.82	0.0023	$h = 0$
4	infiltration	hollow cylindrical	silty clay	−100	1	1.44	0.0400	$h = 0$
5	drainage	rectangular	silty clay	0	5	3	0.0476	$q = 0$

[a]In all scenarios, profile depth = 80 cm, fracture pore system = sand (see Table 1 for van Genuchten parameters), b = 0.25 cm, seepage face lower boundary condition.
[b]See Table 1 for van Genuchten parameters.
[c]Initial pressure head.

reference transfer rate, with the second-order DPM matching closer to the transfer peaks. The good approximation of the first-order term is due to the relatively fast transfer reaching quickly its "late-time" phase for which the first-order term is accurate [*Zimmerman et al.*, 1993].

3.2.3. Effect of a Cylindrical Macropore With the Large Matrix Mantle (Scenario 3)

[28] The cylindrical macropore occupied only 0.23% of the dual-permeability medium (w_f = 0.0023, Table 3) in this scenario as compared with the first scenario where for the same values of a (5 cm) and b (0.25 cm), the fracture between plate-like matrix blocks occupied 4.76% of the domain (w_f = 0.476, Table 3). Figure 13c shows depth profiles of simulated water transfer, Γ_w. In scenario 3 the first-order DPM gave a slightly closer representation of the reference transfer profiles than the second-order DPM. Note that the first-order term is specifically suited for hollow cylindrical systems. For instance, it described solute diffusion in a hollow cylindrical system better as compared with other geometries [*van Genuchten and Dalton*, 1986].

3.2.4. Effect of a Cylindrical Macropore With the Small Matrix Mantle (Scenario 4)

[29] A matrix mantle radius a of only 1 cm resulted in a macropore volume fraction w_f of 0.04, thus being 17 times larger than in scenario 3. Figure 13d shows depth profiles of water transfer Γ_w at 60 and 180 min as simulated using HYDRUS-2D, and the first- and second-order DPMs. Reference transfer profiles revealed faster infiltration in spite of larger transfer than was found for scenario 3 with a equal to 5 cm (compare Figures 13c and 13d). This can be explained by the larger macroporosity w_f for a equal to 1 cm. The second-order DPM approximated the sharply peaked reference transfer profiles considerably better than the first-order DPM.

3.2.5. Effect of Flow Direction: Drainage (Scenario 5)

[30] Finally, a draining scenario is analyzed assuming a soil system similar to scenario 1. The initially saturated profile was subject to a seepage face lower boundary condition and a flux upper boundary condition representing evaporation from the matrix at 0.3 cm/d. Figure 13e shows that the fracture-to-matrix (positive) transfer took place after 60 min in the upper part of the soil profile where evaporation resulted in more negative pressure heads in the matrix than in the fracture. Simultaneously, the matrix-to-fracture transfer occurred in the lower part of the soil profile where fast draining of the macropore caused pressure heads in the macropore to drop below the corresponding values in the adjacent matrix. The overall transfer rates are an order-of-magnitude lower than in the first scenario (compare Figures 13e and 13a). After 600 min, pressure heads in two regions equilibrated near the soil surface, and thus water transfer between the domains approached zero (Figure 13f). Both the first- and second-order DPMs approximated the reference transfer profiles satisfactorily.

[31] Scenarios 1 and 2 demonstrated the significantly higher accuracy of the second-order model for infiltration into a dual-permeability medium of rectangular matrix slabs separated by parallel fractures. As mentioned above, the second-order term was derived for spherical blocks and has been demonstrated to be also applicable to relatively similar geometries as cubes [*Zimmerman et al.*, 1993, 1996]. For infiltration into a cylindrical system with large outer-to-inner-radius ratio, ζ_0 (scenario 3), the second-order term did not give satisfactory results. It was documented in the literature that the exact analytical solution for spherical diffusion fails to describe diffusion in a cylindrical macropore system, even when the geometry is embedded in factor β [*van Genuchten and Dalton*, 1986]. The geometry factor β accounts for the smaller surface-to-volume ratio of the cylindrical macropore system as compared with spheres [*Gerke and van Genuchten*, 1996], but it cannot always compensate for the fundamentally different flow field in the cylindrical macropore system. At early times, the normalized water uptake is proportional to the surface-to-volume ratio. The hollow cylinder has a small surface-to-volume ratio (reflected by a small value of β) particularly for a large outer-to-inner-radius ratio, ζ_0 [*Gerke and van Genuchten*, 1996], and so it will initially have a much smaller water uptake than a sphere (cube, solid cylinder). Only at late times will the flux be nearly the same for the hollow cylinder and the sphere. However, the fourth scenario indicated that the second-order term derived for spherical geometry can be applied to a cylindrical macropore system with small ζ_0, i.e., increasing values for surface-to-volume ratio and β.

[32] For soil systems with small macroporosity, a different transfer equation may be needed. Unfortunately, analytical solutions for diffusion in hollow cylindrical systems [e.g., *van Genuchten et al.*, 1984] are mathematically rather complicated, such that a procedure as that presented by *Vermeulen* [1953] to derive a second-order expression for diffusion into spheres may not be easily applicable for the hollow cylindrical system.

[33] The primary significance of the water transfer calculation might be its effect on advective solute transfer which in dual-permeability models is calculated as

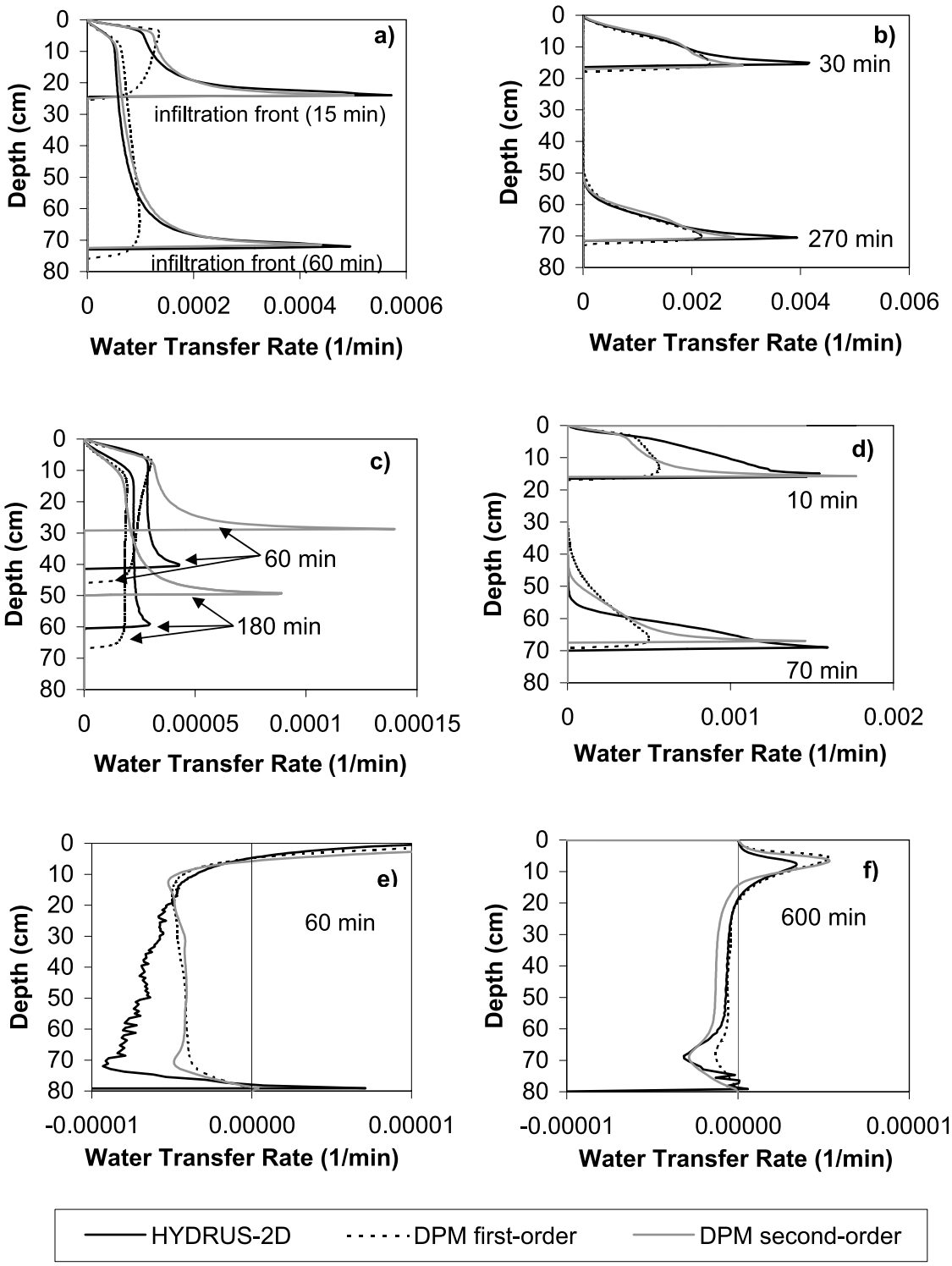

Figure 13. Water transfer rate versus depth as calculated with the two-dimensional (HYDRUS-2D) model, and the dual-permeability model with the first- (DPM first-order) and second-order (DPM second-order) water transfer terms using evaluation scheme (13) with $p = 17$ (weighted arithmetic). Infiltration into dual-permeability medium with (a) silty clay and (b) silt matrix slabs of a half width of 5 cm; infiltration into cylindrical dual-permeability medium with silty clay matrix mantle of (c) 5 cm and (d) 1 cm; drainage and evaporation out of dual-permeability medium with silty clay matrix slabs of 5-cm half width at (e) $t = 60$ min and (f) $t = 600$ min.

water transfer times concentration [e.g., *Gerke and van Genuchten*, 1993b]. A detailed analysis of the impact of advective solute transfer on the simulation of preferential solute transport, however, is beyond the scope of this study and will be addressed in a separate paper.

4. Concluding Remarks

[34] A second-order term originally derived for water transfer between fractures and matrix in fractured rock was adapted for variably saturated structured soils. The hydraulic conductivity in the second-order term was evaluated as a weighted average function of pressure heads in the matrix and fracture. This modification significantly improved agreement between water transfer calculated with the second-order term and a numerical solution of a reference equation for horizontal flow. A single weighting factor of 17 proved successful to describe water transfer for a range of initial and boundary conditions, as well as for different soil matrix block sizes and textures. Furthermore, the initial pressure head in the second-order term was treated as a dynamic parameter to be reset upon change of flow direction between matrix and fracture domains. With this adjustment the second-order term does not show pseudohysteresis for varying directions of water transfer, as opposed to the second-order term with constant initial pressure head and the first-order term with scaling factor. Implemented in a dual-permeability model, the modified second-order transfer term improves the accuracy of preferential soil water flow simulations as compared with a first-order term, particularly for geometries other than hollow cylinders. The modified second-order term is as versatile as first-order terms with regard to its application in dual-permeability models for studying variably saturated flow in field soils.

[35] **Acknowledgment.** This work was supported by the National Science Foundation (grant EAR 0296158 and STC Program, EAR 9876800).

References

Carsel, R. F., and R. S. Parrish (1988), Developing joint probability distributions of soil water retention characteristics, *Water Resour. Res.*, *24*, 755–769.

Dykhuizen, R. C. (1990), A new coupling term for dual-porosity models, *Water Resour. Res.*, *26*, 351–356.

Gerke, H. H., and M. T. van Genuchten (1993a), Evaluation of a first-order water transfer term for variably saturated dual-porosity flow models, *Water Resour. Res.*, *29*, 1225–1238.

Gerke, H. H., and M. T. van Genuchten (1993b), A dual-porosity model for simulating the preferential movement of water and solutes in structured porous media, *Water Resour. Res.*, *29*, 305–319.

Gerke, H. H., and M. T. van Genuchten (1996), Macroscopic representation of structural geometry for simulating water and solute mass transfer in dual-porosity media, *Adv. Water Resour.*, *19*, 343–357.

Green, I. R. A., and D. Stephenson (1986), Criteria for comparison of single event models, *Hydrol. Sci.*, *31*(3), 395–411.

Gwo, J. P., P. M. Jardine, G. V. Wilson, and G. T. Yeh (1995), A multiple-pore-region concept to modeling mass transfer in subsurface media, *J. Hydrol.*, *164*, 217–237.

Ray, C., T. R. Ellsworth, A. J. Valocchi, and C. W. Boast (1997), An improved dual porosity model for chemical transport in macroporous soils, *J. Hydrol.*, *193*, 270–292.

Simunek, J., M. Sejna, and M. T. van Genuchten (1998), The HYDRUS-1D software package for simulating the one-dimensional movement of water, heat, and multiple solutes in variably-saturated media, version 2.0, *Rep. IGWMC-TPS-70*, 202 pp., Int. Ground Water Modell. Cent., Colo. School of Mines, Golden, Colo.

Simunek, J., M. Sejna, and M. T. van Genuchten (1999), The HYDRUS-2D software package for simulating two-dimensional movement of water, heat, and multiple solutes in variably-saturated media, version 2.0, *Rep. IGWMC-TPS-53*, 251 pp., Int. Ground Water Modell. Cent., Colo. School of Mines, Golden, Colo.

Simunek, J., N. J. Jarvis, M. T. van Genuchten, and A. Gärdenäs (2003), Review and comparison of models for describing nonequilibrium and preferential flow and transport in the vadose zone, *J. Hydrol.*, *272*, 14–35.

van Genuchten, M. T. (1980), A closed-form equation for predicting the hydraulic conductivity of unsaturated soils, *Soil Sci. Soc. Am. J.*, *44*, 892–898.

van Genuchten, M. T., and F. N. Dalton (1986), Models for simulating salt movement in aggregated field soils, *Geoderma*, *38*, 165–183.

van Genuchten, M. T., D. H. Tang, and R. Guennelon (1984), Some exact solutions for solute transport through soils containing large cylindrical macropores, *Water Resour. Res.*, *20*, 335–346.

Vermeulen, T. (1953), Theory of irreversible and constant-pattern solid diffusion, *Ind. Eng. Chem.*, *45*, 1664–1670.

Warren, J. E., and P. J. Root (1963), The behavior of naturally fractured reservoirs, *Soc. Pet. Eng. J.*, *3*, 245–255.

Young, D. F., and W. P. Ball (1997), Effects of column conditions on the first-order rate modeling of nonequilibrium solute breakthrough: Cylindrical macropores versus spherical media, *Water Resour. Res.*, *33*, 1149–1156.

Zimmerman, R. W., G. Chen, T. Hadgu, and G. S. Bodvarsson (1993), A numerical dual-porosity model with semianalytical treatment of fracture/matrix flow, *Water Resour. Res.*, *29*, 2127–2137.

Zimmerman, R. W., T. Hadgu, and G. S. Bodvarsson (1996), A new lumped-parameter model for flow in unsaturated dual-porosity media, *Adv. Water Resour.*, *19*(5), 317–327.

H. H. Gerke, Center for Agricultural Landscape and Land Use Research (ZALF), Institute of Soil Landscape Research, Eberswalder Strasse 84, D-15374 Müncheberg, Germany. (hgerke@zalf.de)

J. M. Köhne and B. P. Mohanty, Department of Biological and Agricultural Engineering, Texas A&M University, 140 Scoates Hall, College Station, TX 77843-2117, USA. (mkoehne@cora.tamu.edu; bmohanty@tamu.edu)

J. Simunek, Department of Environmental Sciences, University of California, Riverside, 900 University Avenue, A135 Bourns Hall, Riverside, CA 92521, USA. (jiri.simunek@ucr.edu)